Size-Dependent Phase Transition of Diamond to Graphite at High Pressures

ARTICLE *in* THE JOURNAL OF PHYSICAL CHEMISTRY C · SEPTEMBER 2007

Impact Factor: 4.77 · DOI: 10.1021/jp073576k

Size-Dependent Phase Transition of Diamond to Graphite at High Pressures

V. A. Davydov,*,† A. V. Rakhmanina,† S. Rols,‡ V. Agafonov,§ M. X. Pulikkathara,|| R. L. Vander Wal,⊥ and V. N. Khabashesku*,||

L. F. Vereshchagin Institute for High Pressure Physics of the RAS, Troitsk, Moscow region, 142190, Russia, Institut Laue-Langevin, 38042 Grenoble Cedex, France, L.E.M.A., UMR CNRS-CEA 6157 - LRC CEA M01, Université François Rabelais, av. Monge 31, Tours, 37200, France, Department of Chemistry and Richard E. Smalley Institute for Nanoscale Science and Technology, Houston, Texas 77005-1892, and The National Center for Microgravity Research, NASA Glenn Research Center, 2100 Brookpark Road, MS 110-3, Cleveland, Ohio, 44135

Received: May 10, 2007; In Final Form: July 11, 2007

Size-dependent phase transition of nanosize diamond particles (NDPs) to graphite was found in the course of studies of high pressure high temperature (HPHT) induced transformations of NDPs at 8 GPa and in the temperature range of 873−1623 K. Analysis of the products of HPHT treatment of powder NDPs (with the mean size of 4.5 nm) by X-ray diffraction (XRD), scanning (SEM) and transmission electron (TEM) microscopies, and Raman spectroscopy have shown that at 8 GPa the increase of the treatment temperature results in a gradual enlargement of NDPs. According to XRD data, the temperature increase from 873 to 1473 K at the treatment time of 60 s gives rise to NDP mean size enlargement from initial 4.5 to 8.8 nm. However, the largest NDPs can reach the sizes of 13.5−14.0 nm at 1473 K, as measured directly from TEM images. At 1623 K, size-dependent phase transition of diamond to graphite has been observed. By applying the Arrenius equation to the particle mean size versus treatment temperature plot, activation energy for the diamond solid phase growth at 8 GPa was calculated to be 112 ± 8 kJ/mol. The critical size of NDP corresponding to the point of phase transition at 8 GPa and 1623 K was estimated to be ∼18 nm. The likely effect of the size-dependent diamond-to-graphite phase transition on the process of diamond synthesis and, in particular, the problem of formation of critical seeds for crystal growth of macroscale diamond are discussed in the paper.

Introduction

The problem of relative stability of various nanosize forms of carbon has attracted a lot of attention in the last 10−15 years. Theoretical analysis of size stability of different linear-, planar-, ring-, and sphere-shaped structural isomers as well as three-dimensional clusters with the diamond and graphitic structures[1−13] has shown that the size-dependent phase transformation is a distinctive feature of the nanoscale carbon system. Ring-shaped structures, in particular, are expected to be the most stable form of carbon clusters made of about 20 atoms.[2] With the higher number of atoms in the cluster, the sphere-shaped structure becomes energetically more favorable. This result was obtained for the isomers of C_{24}, C_{26}, C_{28}, and C_{32} cluster series for which the fullerene-type structures appeared to be more stable than the ring-shaped ones.[4] According to molecular dynamics calculations,[5] the most stable isomer of the C_{360} cluster has a thoroid-shaped structure which suggests a possibility for transformation of fullerene into the thoroidal form of carbon. The same level calculations have also demonstrated the likelihood of transformation of NDPs, comprised of 150 or more atoms, into a double-walled onion-like structures at temperatures of 1400−2800 K.[6]

The size-dependent diamond-to-graphite phase transformation has been the most studied theoretically.[7−13] The thought that at the nanoscale the diamond phase could be more stable than graphite even at low pressures was mentioned earlier, in 1960s−1970s, in view of the successful synthesis of diamond under conditions of its metastability realized during deposition of carbon from the gas phase.[14] The same concept was applied to explain the existence of diamond nanoparticles (∼5 nm size) in the unshocked meteorites.[7] Preparation of the same size (2−7 nm) NDPs through a different synthetic methodologies, such as explosion of carbon materials,[15,16] implantation of carbon ions into a quartz substrate,[17] high pressure high temperature (HPHT) treatment of multiwalled carbon nanotubes,[18] and laser vaporization of graphite,[19] has led to an assumption that the nanosize range produced most likely represents the window of thermodynamic stability of diamond.

Calculations of the potential energy changes for diamond and graphite nanoparticles depending on carbon cluster size, done by different approaches, assisted in obtaining different estimations of the maximum size of diamond cluster for size-dependent diamond-to-graphite phase transition in the low-pressure region at 0 K. According to different theoretical models, the maximum size (d) of NDPs stable under these conditions is equal to 3 nm,[8] 0.6−1.4 nm,[9] 15 nm,[10] ∼5.9 nm,[11] 5.2 nm,[12] and 13.5 nm.[13] The most complete theoretical analysis so far of the problem of size-dependent phase transitions in the carbon system is probably given in refs 12 and 13 which considered up to 5 forms of nanosized carbon, fullerenes, onions, bucky diamond,

* Corresponding authors: vdavydov@hppi.troitsk.ru; khval@rice.edu.
† L. F. Vereshchagin Institute for High Pressure Physics of the RAS.
‡ Institut Laue-Langevin.
§ Université Francois Rabelais.
|| Richard E. Smalley Institute for Nanoscale Science and Technology.
⊥ NASA Glenn Research Center.

10.1021/jp073576k CCC: $37.00
Published on Web 08/14/2007 PAGE EST: 7.1

graphite, and diamond nanoparticles. According to the $d-T$ (size−temperature) diagram created for these forms of carbon in the temperature range of 0−1500 K and pressure $P = 0$ GPa,[13] each form of nanocarbon shows its own size range of thermodynamic stability. At 0 K, these critical sizes are 0−2.5 nm for fullerenes, 2.5−2.7 nm for onions, 2.7−9.0 nm for diamond, and >13.5 nm for graphite. The temperature increase was predicted to cause a considerable change of the phase boundary size only in the case of a diamond-to-graphite transformation for which the critical size of NDPs decreased from 13.5 nm at 0 K to 4.3 nm at 1500 K.

Unlike theoretical studies, the experimental work on interconversions of different nanoscale forms of carbon was carried out thus far mostly on diamond and onions.[20−30] It involved either thermal stability studies of different size fractions or stability of the nanoparticles under high-energy electron[28] or laser[30] irradiation and did not particularly focus on size-dependent phase stability of these carbon forms.

Transmission electron microscopy (TEM) studies of NDPs ($d \sim 5$ nm), annealed at high temperatures in vacuum, have demonstrated that nanodiamond converts into spherical onion-like particles at temperatures of 1370−1870 K.[20] The conversion process initiates from the diamond surface gradually moving toward the core of the nanoparticle. Therefore, at some intermediate stages, the process yields nanoparticles having diamond nuclei and onion-like outer shell. These particles, called bucky diamonds, are occasionally even considered as a new form of carbon.[12] Follow-up studies[21] of the kinetics of graphitization of nano- and submicron-size diamond have indicated that the starting temperature for diamond graphitization depends on particle size being about 1370 and 1920 K for nano- and submicron-size diamond, respectively. It was also shown that full conversion of diamond into spherical onion-like particles occurs for the NDPs with initial size smaller than 2 nm already at $T \sim 1420$ K and for those with 5−6 nm size only at $T \sim 1920$ K and higher. Above 1920 K, the processes lead to the formation of polyhedral particles with closed carbon shells. Diamond nuclei completely disappear under these conditions. Thus, an increase in the treatment temperature of NDPs leads to the following sequence of transformations: nanodiamond → bucky diamond → spherical onion-like particles → polyhedral particles and graphitic ribbons.

These results[20,21] have been confirmed by other groups.[22−27] X-ray diffraction and TEM studies[24,25] showed that NDPs ($d \sim 5$ nm) under thermal treatment at temperatures below 1973 K convert into spherical onion-like particles, having nearly the same size as the starting nanodiamond particles. At higher temperatures (∼2273 K), notably larger size hollow polyhedral particles are formed as the main product. It was also found[24,25] that even at temperatures below 1673 K the smallest size NDPs already undergo transformation. The similar size-dependent relationship with the graphitization starting temperature was observed in the work of Qiao et al.[26] It was proposed that the driving force for the transformation of diamond cluster into spherical onion-like particle, which can be marked by the "onionization" term, is the reduction of the number of free carbon bonds in the system through formation of closed graphene networks which minimizes the surface energy of the particle.[27]

The recent studies have also demonstrated the possibility of a reverse onion-to-diamond transformation, yet under special conditions involving irradiation of onions by a high-energy electron beam at $T \sim 973$ K,[28] ion bombardment (MeV, Ne^+),[29] or lasers.[30] The spherical onion-like particles were also observed to convert into diamond under thermal treatment in air for 180 min at 773 K in absence of any type of irradiation.[31] However, it was suggested,[31] that this transformation should not be considered as a direct transition between two nanosize phases of carbon because of the special role played by oxygen present in the system. According to the proposed mechanism,[31] oxygen etches mainly the stressed sites on the onions creating many vacancies which facilitate the formation of the diamond structure.

In the earlier experimental work, studies of the pressure effect on direct transformations of different nanoscale forms of carbon in regard to the problem of thermally induced graphitization of NDPs under pressure and the related problem of their sintering have also been carried out. However, observation of size-dependent phase transformations has not been the goal of these studies.

In the most detailed study[32] of the effect of high pressure on graphitization of nano- and submicron-size diamond powders in the temperature range of 973−1673 K, it was shown that at constant pressure, temperature, and treatment time the extent of diamond graphitization is essentially controlled by the size of diamond particles. The maximum conversion (up to 100%) was found for the smallest size diamond particles with the average size $d \sim 5$ nm, while the minimum change occurred for the largest submicron size fractions ($d \sim 30-40$ μm). The activation energies for graphitization were found to be 202 kJ/mol for ∼5 nm size diamond particles and 365 kJ/mol for those having the average size of about 35 μm. Pressure is the second most critical parameter effecting the graphitization (onionization) of diamond nanoparticles. According to Qian et al.,[32] graphitization of 5 nm size NDPs at 2 GPa, 1473 K, and 30 min leads to formation of the hollow polyhedral 5−10 nm size particles and not to formation of spherical nanostructures which are produced under vacuum conditions. The increase of pressure leads to suppression of the graphitization process in such a way that the smaller size diamond particles require a higher pressure for the suppression of their graphitization. In particular, it was found that during the 60 s treatment of the smallest NDPs ($d \sim 5$ nm) at 1473 K, pressure increased from 2 to 8 GPa which results in a dramatic change of the degree of diamond graphitization from 100% at 2 GPa to 0% at 8 GPa, meaning a total suppression of this process at 8 GPa for even the smallest size nanoparticles.[32]

Studies of the sintering process of diamond nanopowders at 4.5−7.0 GPa and 1673 K have confirmed the occurrence of suppressed graphitization of NDPs by high pressures and have shown that the thermal treatment of NDPs under pressure can lead to a distinct enlargement of the mean size of primary nanoparticles.[33]

By taking into account the fact that thermal treatment of NDPs at 7−8 GPa under the conditions of suppressed graphitization and onionization of these nanoparticles can lead to their enlargement, in the present work, we have attempted studies of size-dependent transformations of NDPs at 8 GPa in order to find an experimental proof for the possibility of a theoretically predicted size-dependent phase transition of diamond into graphite.[10−13]

Experimental Section

Powder of NDPs (Nanostructured and Amorphous Materials, Inc) with the mean particle size of 4.5 nm was used as a precursor material in the present work. Energy dispersive X-ray (EDX) elemental analysis of this powder has shown the presence of the following impurities: O (2 atom %), Fe (0.1−0.15%), Si (0.1−0.3%), Na (0.15%), and S (0.14%). The HPHT

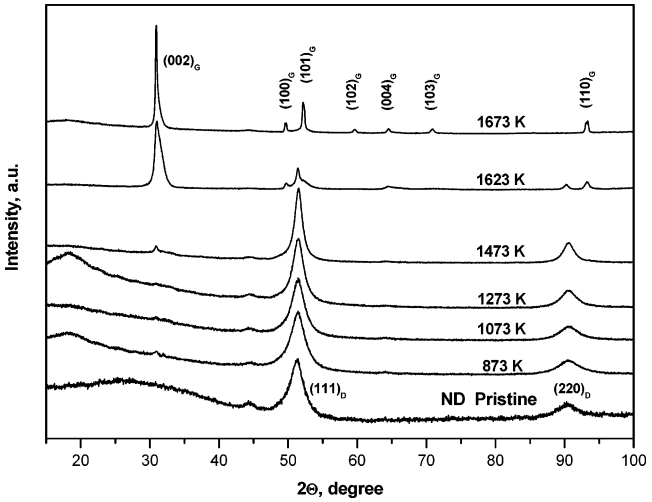

Figure 1. X-ray diffraction patterns of the pristine nanosize diamond powder and the products of its treatment at 8 GPa and different temperatures.

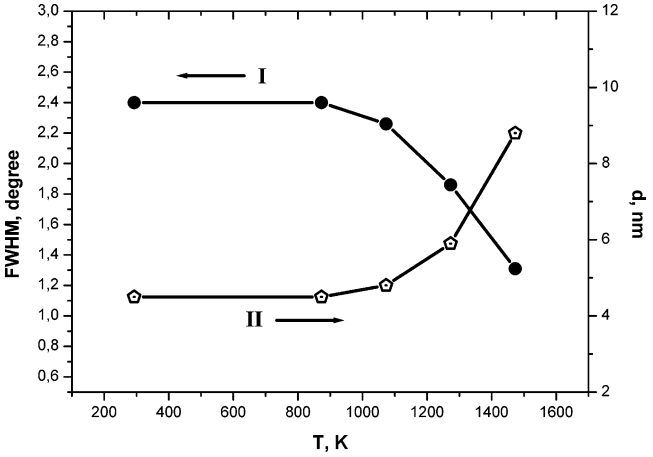

Figure 2. Temperature dependences of fwhm of the (111) diamond diffraction peak (I) and average particle size (*d*) value (II) plotted for the samples produced by HPHT treatment of diamond nanoparticles with the average size of 4.5 nm at 8 GPa.

treatments of the nanodiamond powder were carried out in the Toroid-type high pressure apparatus.[34] Cold-pressed pellets of the initial powder (4.5 mm diameter and 3 mm height) have been placed into a central zone of the graphite heater of the high pressure apparatus. The experimental procedure involved loading of the apparatus to the pressure of 8.0 GPa at room temperature, followed by the heating (with a heating rate of 15°/s) and isothermal holding of the samples at temperatures of 873, 1073, 1273, 1473, 1623, and 1673 K during 60 s exposure time under a constant load, then fast cooling of the apparatus to room temperature completed by slow unloading. The temperature measurements were taken directly on the side surface of the sample by using chromel−alumel and Pt−Pt/Rh thermocouples. The relative accuracy of the temperature measurements was ±2°; however, for the temperatures above 1473 K, the absolute accuracy was ±50°.

The samples of the high pressure states, obtained as pellets, were taken out from the apparatus and characterized by X-ray diffraction (XRD), transmission and scanning electron microscopies (SEM), and micro-Raman spectroscopy. XRD data were collected on an INEL CPS 120 powder diffractometer using a Co $K\alpha_1$ radiation source. The Raman spectra were collected with a Renishaw 1000 microraman system operating with a 514 nm argon laser source. Microscopy studies were carried out with DSM 982 Gemini (Zeiss) scanning electron microscope and transmission electron microscopes JEM-1230 (JEOL) and Phillips CM20 with Gatan image filter of 0.14 nm resolution at accelerating voltages of 120 and 200 kV, respectively. Samples for TEM studies were prepared by sonication assisted dispersion in ethanol for 15 min. The obtained suspension was deposited onto a lacey carbon coated copper grid and then dried in air.

Results and Discussion

X-ray Diffraction Analysis. Figure 1 shows the evolution of the XRD patterns for the high pressure states in relation to the treatment temperature of the initial nanosize diamond powder. According to XRD data, the initial powder contains nanodiamonds (as shown by (111) and (220) reflections on Figure 1) and some quantities of the disordered carbon forms which is witnessed by the appearance of a broad band with the maximum centered near 26.5° and an additional small diffuse peak at 44.3°. The diffuse character of these bands precludes the explicit identification of carbon impurities. Presumably, they are composed of a mixture of disordered carbon forms and small carbon clusters built mainly from regular and distorted sp^2 state carbons structurally organized into a planar or rolled graphene segments.

Comparative analysis of XRD patterns of the samples prepared at different temperatures shows that the increase in treatment temperature in the range of 873−1473 K causes a gradual thinning of the diffraction peaks of diamond. This indicates the enlargement of the mean size of diamond nanoparticles with the temperature increase. The relationship between the XRD (111) line width (full width at half-maximum, fwhm) of diamond and the temperature in the range of 873−1473 K is plotted in Figure 2. By applying the Scherrer equation to the (111) line broadening values, the mean particle size (*d*) was estimated for the starting diamond powder (4.5 ± 0.1 nm) and for the samples produced at different temperatures. The relationship between diamond nanoparticle mean size and treatment temperature determined by this procedure is also shown in Figure 2. According to these data, the temperature increase from 873 to 1473 K results in the nanoparticle mean size enlargement from the initial 4.5 to 8.8 nm. The content of weakly ordered carbon fraction becomes reduced in this case which means that this fraction is consumed in the process of diamond particles build-up and partially by formation of small size sets of graphene layers weakly ordered three-dimensionally. The presence of a small quantity (about a few percent) of these carbon formations in the products of nanodiamond treatment under the temperature range of 873−1473 K is evident from the XRD patterns. They show the appearance of weak features near 30.8 and 63.8°, close to positions of (002) and (004) reflections in the diffractogram of graphite (Figure 1).

In the XRD of the sample treated at temperature of 1623 K, the intensities of diamond diffraction peaks were observed to considerably weaken while several reflections with the maxima positions corresponding to the diffraction peaks of graphite were observed to appear. The presence of distinct three-dimensional (100) and (101) peaks of graphite in the diffractogram of the sample, produced by treatment of diamond at 1623 K, provide evidence for a substantially high degree of three-dimensional (3D) ordering within the sets of graphene layers formed. Mean sizes of the graphite crystallites (L_a and L_c), formed at 1623 K, were estimated from the XRD data[35] and found to be $L_a = 53$ nm and $L_c = 28$ nm, where L_a is the crystallite size within the

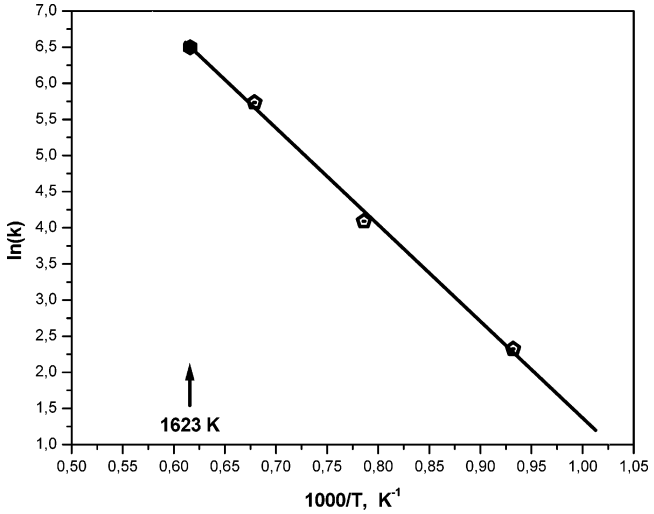

Figure 3. Temperature dependence of the constant of diamond growth rate at 8 GPa. The black square denotes the value of the rate constant at temperature of 1623 K which corresponds to the temperature of size-dependent phase transition of diamond to graphite.

graphene plane and L_c is the size in the direction perpendicular to graphene plane.

In the XRD of the sample treated at the highest temperature, 1673 K, only the peaks of graphite were observed (Figure 1). These data indicate that at the XRD analysis detection level graphite is the dominant product of the transformation of diamond at 8 GPa and 1673 K. The graphite particles formed in this process are not of nanosize but of submicrometer and micrometer dimensions.

The obtained relationship between the mean size of diamond particles and treatment temperature (Figure 2) allowed for estimation of the activation energy for the enlargement process of diamond nanoparticles at 8 GPa. The chart showing the dependence of rate constant of the enlargement process versus reversed temperature is given in Figure 3. By applying the Arrenius equation to this chart, the activation energy (E_a) for the enlargement process of diamond nanoparticles at 8 GPa was found to be 112 ± 8 kJ/mol. The experimental data shown in Figure 3 also allow estimation of the mean size of NDPs at 1623 K, which is equal to 11.1 ± 2.0 nm.

The XRD analysis provided the most representative data for bulk characterization of the system. However, these data have also been complemented by using the methods of microscopic analysis such as micro-Raman spectroscopy and scanning and transmission electron microscopies.

Figure 4 shows Raman spectra in the 1200−1750 cm^{-1} region for the initial nanodiamond powder and samples obtained by its treatment at 8 GPa and different temperatures. The Raman spectrum of the initial powder shows two bands at 1326 and 1625 cm^{-1}. The first band is typical of nanosize diamond consisting of small atomic clusters of ordered sp^3 bonded carbon. In comparison with the position of the Raman peak of monocrystalline bulk diamond at 1332.5 cm^{-1} with the bandwidth (fwhm) of 2 cm^{-1},[36] the band of NDP is down-shifted and asymmetrically broadened to fwhm of 41 cm^{-1}. The observed effect of diamond cluster size on position and shape of spectral band can be explained with the help of phonon confinement model.[37−41] By using this model and values of the *A* and *B* coefficients for the phonon dispersion curves of diamond near the center of Brillouin zone ($q \sim 0$), $A = 1241.25$ cm^{-1}, $B = 91.25$ cm^{-1}, suggested by Ager et al.,[38] we have estimated the mean size of NDPs to be 4.5 nm which agrees

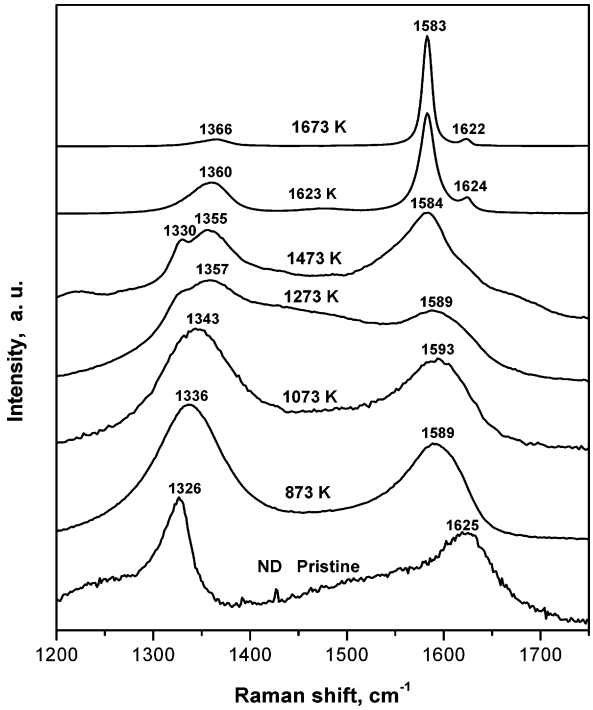

Figure 4. Raman spectra of the pristine nanosize diamond powder and products of its treatment at 8 GPa and temperatures of 873, 1073, 1273, 1473, 1623, and 1673 K.

with the value obtained from the X-ray diffraction. The observed broad band at 1625 cm^{-1} indicates the presence of weakly ordered clusters of sp^2 state carbons in the initial powder confirming the X-ray analysis data. In part, these clusters are present as an impurity in the initial powder and partly as a constituent of the outer shells of nanoparticles creating bonded sp^2/sp^3 state carbons. It should be noted that the upshift to 1625 cm^{-1} of the band of sp^2 state carbons provides an indirect evidence for presence in the system of not only aromatic but also isolated C═C double bonds.[42,43] The latter are shorter than aromatic bonds and show higher vibrational frequencies.

Treatment of initial powder under pressure of 8 GPa and different temperatures produces significant changes in the Raman spectra of samples. According to X-ray data, treatment at 873 K does not change the initial mean size of NDPs. At the same time, notable changes in the low angle (<45°) section of the diffractogram are observed, such as weakening of the broad diffuse band at 26.5° and appearance of a small but detectable peak at 30.8°, close to the position of (002) reflection of graphite. These data show that the transformations in the system occur mainly at the expense of sp^2 state bonded carbons. Raman spectra provide additional information on this process. According to thermal gravimetric analysis of the initial diamond nanopowder, the detachment of surface covalently bonded functional groups and evolution of volatile products starts at a temperature near 873 K. This involves significant reconstruction of the NDP surface through the creation of weakly ordered clusters of sp^2 carbons which are closing the dangling sp^3 carbon bonds being formed during the desorption of surface bonded species. Studies of thermally induced transformations of NDPs in vacuum[40] have shown that the desorption process is followed by appearance in the Raman spectrum of two broad bands at ∼1350 and 1580−1600 cm^{-1}, designated as D "disorder-induced" and G "graphitic" bands.[44] The most significant change observed in the Raman spectrum of the sample treated at 8 GPa

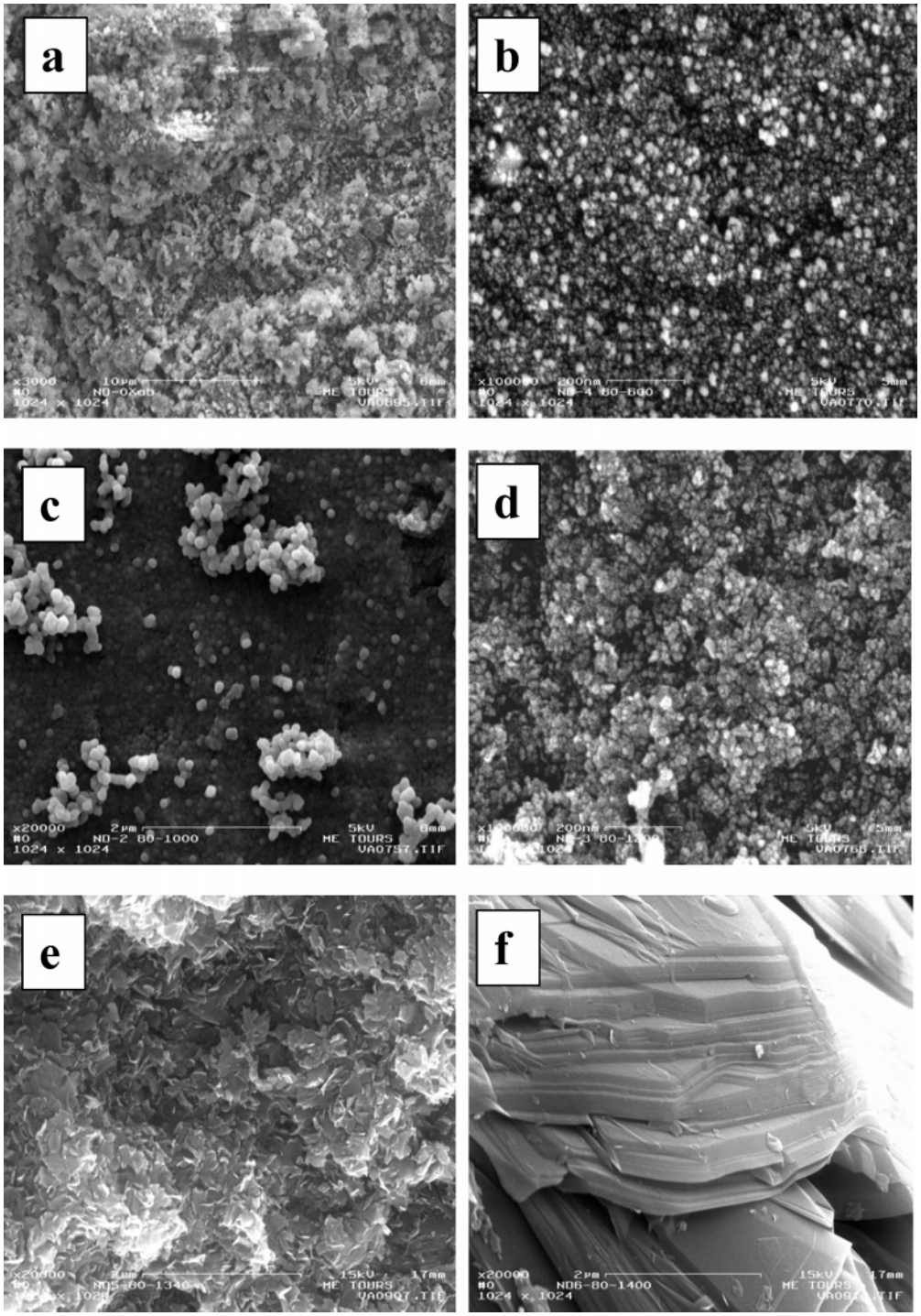

Figure 5. SEM micrographs of the pristine nanosize diamond powder (a) and products of its treatment at 8 GPa and temperatures of 873 (b), 1273 (c), 1473 (d), 1623 (e), and 1673 K (f).

and 873 K is the downshift to 1590 cm^{-1} of the band of the sp^2 state carbons relatively to 1625 cm^{-1} position in the spectrum of initial nanopowder (Figure 4). Shift to the 1580−1600 cm^{-1} region, typical for the G band of graphite (E_{2g} vibrational mode[44]), indicates an increase of a relative amount of two-dimensionally ordered sp^2 state carbons first of all at the expense of carbon atoms initially bonded to either surface functionalities or C═C double bonds. In addition, substantial broadness of the G band points at the small size and defectiveness of the graphene segments which compose graphite-like clusters.

Presence of this type of clusters is normally accompanied by appearance of broad D bands near 1350 cm^{-1}. In the spectrum of sample, produced at 873 K, a broad band at 1336 cm^{-1} is observed. Deconvolution of this band including asymmetric feature of nanosize diamond peaking at 1326 cm^{-1} indeed results in the separation of the second contributing component with the peak maximum at 1353 cm^{-1}. Taking into account that Raman scattering cross section of diamond is about one-sixtieth of graphite,[45] we find that the position of the overlapped band maximum at 1336 cm^{-1} shows that the content of the sp^2 state carbons in the sample treated at 873 K is quite low. On the other hand, existence of such superposition precludes the use of Raman data for quantitative description of the relationship between nanoparticle size and treatment temperature.

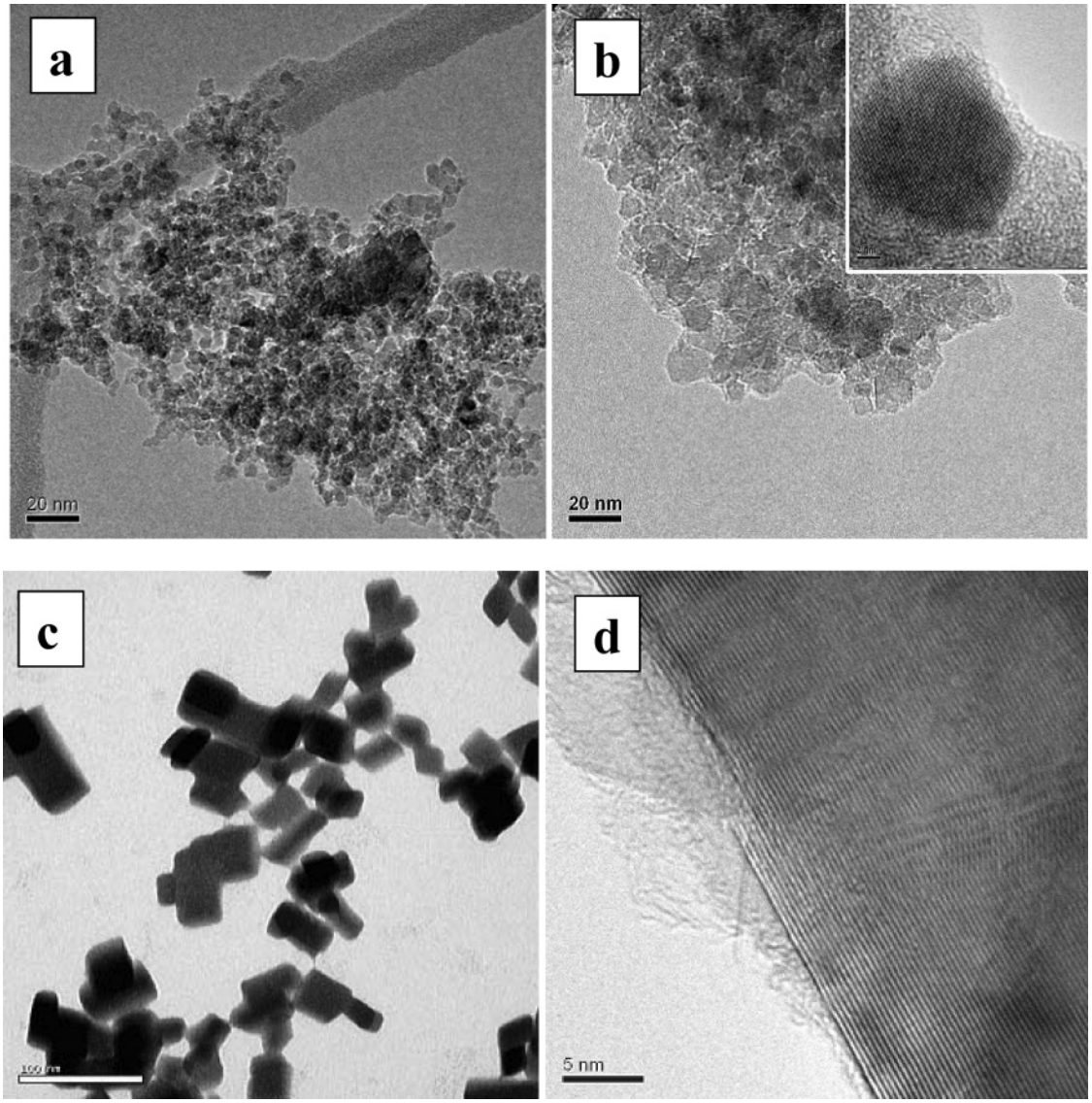

Figure 6. TEM images of the pristine nanosize diamond powder (a) and products of its treatment at 8 GPa and temperatures of 1473 (b) and 1623 K (c, d).

Increase of the treatment temperature to 1473 K, which according to XRD data causes the enlargement of NDPs size, results in further enhancement of the sp^3 state carbon ratio in the sample. This is indicated by appearance in the Raman spectra of the band of nanosize diamond at 1330 cm^{-1} which at 1073 K appears as a rather weak feature, to become significant at 1273 K, and clearly detectable at 1473 K. The observed shift of the band position maximum of nanosize diamond from the initial 1326 cm^{-1} to 1330 cm^{-1} agrees quite well with the phonon confinement model.

Raman spectra of the samples, produced at 1623 and 1673 K, unambiguously confirm formation of graphite particles. The size and degree of crystallinity of these particles develop with the increase of treatment temperature.

SEM micrographs of initial diamond nanopowder and break-off samples, produced via treatment of this powder at 8 GPa and temperatures of 873, 1273, 1473, 1623, and 1673 K, are shown in Figure 5. According to SEM, all samples, produced at 8 GPa and temperature range of 873−1473 K, exhibit virtually identical images of the agglomerates of individual grains of NDPs (Figure 5b−d). Unlike them, the sample prepared at 1623 K shows a drastically different image (Figure 5e) representing compacted nanosize flakes of graphite-like material. At 1673 K, these graphite particles enlarge significantly reaching a micrometer scale size, as shown in Figure 5f. At the same time, the particle size enlargement is accompanied by significant improvement in the degree of crystallinity of graphite indicated by appearance of crystal faceting in some particles.

Figure 6 shows the TEM images taken for the pristine (Figure 6a) nanosize diamond powder and products of its treatment at 8 GPa and two temperatures, 1473 K (Figure 6b) and 1623 K (Figure 6c,d). Comparison of the same magnification TEM images given on Figure 6a,b clearly indicates the increase of the mean size of NDPs after their HPHT treatment. On the basis of the XRD data, the estimated mean size enlargement can be presented by the ratio of 8.8 nm/4.5 nm = 1.96. However, the high-resolution TEM image of the individual NDP grain, given in the inset in Figure 6b as an example, shows that at 1473 K the largest diamond particles can reach a size of ∼13.5−14.0 nm. The size of this particle is about 1.6 times larger than the mean size (8.8 nm) calculated from bulk characterization XRD data. Given this fact, it can be assumed that the maximum NDP size value describing a point of diamond-to-graphite phase transition on the size−temperature phase diagram is also 1.6 times larger than the XRD-derived NDP mean size (11.1 ± 2.0 nm) at 1623 K and is equal to ∼18 nm. It is also interesting to

note that the NDPs, obtained in the process of HPHT growth, show no visible outer shells consisting from the sp^2 bonded carbon (Figure 6b).

Figure 6c,d shows the images of particles of carbon materials formed from the NDPs at 8 GPa and 1623 K. The particles shown on these images are drastically different in appearance from those in Figure 6a,b. They are not spherical anymore and appear as platelets of graphite (Figure 6c). The observed graphite particle sizes (Figure 6c) are in good agreement with the sizes determined from the X-ray data. High-resolution TEM imaging (Figure 6d) confirmed a graphitic carbon interlayer d spacing of 0.335 nm in these particles. It is important to note that according to TEM data, spherical onion-like and polyhedral carbon particles, typically formed during thermally induced graphitization of nanodiamond under vacuum and low-pressure conditions,[20,21,24,25,32] are not observed in the products of transformation of nanodiamond at 8 GPa. These data provide additional support to the interpretation of the observed transformation in the present work of nanosize diamond into graphite as a size-dependent phase transition and not just as an ordinary thermally induced graphitization of NDPs. This phase transition, theoretically predicted for a low-pressure range (~1 atm and below), occurs at a pressure as high as 8 GPa, that is in the range of thermodynamical stability of bulk size diamond.

In regard to the mechanisms of the thermally induced transformations of diamond nanoparticles under a high (8 GPa and above) and low (down to vacuum) pressures, it is interesting to compare the activation energy E_a of solid-phase growth of NDPs, estimated in the present work (112 kJ/mol), with the documented E_a values for graphitization (or, more accurately, onionization) of NDPs in the temperature range of 1370−1870 K. On the basis of different studies, these values are 189 kJ/mol for 4.7 nm[21] and 202 kJ/mol for 5 nm size diamond particles.[32] The almost two times higher activation energy for the onionization than for the growth of 5 nm size NDPs most likely becomes a dominating factor for the growth of 4.5−5.0 nm size NDPs as compared with their onionization during a thermal treatment at 8 GPa. The latter is a predominant process for the thermal transformation of these nanoparticles under low pressures. The obtained results allow for the assumption that the solid-phase NDPs growth at 8 GPa can be associated with both coalescence of single NDPs and addition of single carbon atoms or small carbon clusters, being present in the initial powder, to the NDPs. Making an unambiguous conclusion on the real role of these two possible mechanisms in the NDP growth calls for further investigation.

On the basis of the existence of size-dependent phase transformation of diamond to graphite under high pressures, the fundamentally important statement can be made that the diamond particles of ~2−18 nm size cannot become critical seeds for the growth of bulk diamond since the enlargement of diamond nanoparticles should lead to their transformation into graphite. At least, this is true for the diamond growth conditions comparable to those applied in the present work. In the earlier work, we observed formation of diamond nanoparticles during a thermal destruction of hydrocarbons at 8 GPa and 1423 K, which is below the initiation temperature limit (~1553 K) for micrometer scale (5−40 μm) diamond growth from aromatic hydrocarbons at 8 GPa.[36] In light of the results obtained in the present work, this observation looks even more reasonable.

Acknowledgment. This work was supported by the Russian Foundation for Basic Research (Grant 06-03-32050) and in part by Award No. RUE 2-2659-MO-05 of the U.S. Civilian Research and Development Foundation for Independent States of the Former Soviet Union (CRDF). V.A.D. is also grateful for financial support from Le Studium, Agency for Research and Hosting Foreign associated Researchers in the Centre region (France). The authors thank Victoria M. Bryg for obtaining high-resolution TEM images.

References and Notes

(1) Ballone, P.; Milani, P. *Phys. Rev. B* **1990**, *42*, 3201−3204.
(2) Jing, X.; Chelikowski, J. R. *Phys. Rev. B* **1992**, *46*, 15503−15508.
(3) Menon, M.; Subbaswamy, K. R.; Sawtarie, M. *Phys. Rev. B* **1993**, *48*, 8398−8403.
(4) Kent, P. R. C.; Towler, M. D.; Needs, R. J.; Rajagopal, G. *Phys. Rev. B* **2000**, *62*, 15394−15397.
(5) Itoh, S.; Ihara, S.; Ritakami, J. *Phys. Rev. B* **1993**, *47*, 1703−1704.
(6) Fugaciu, F.; Hermann, H.; Seifert, G. *Phys. Rev. B* **1999**, *60*, 10711−10714.
(7) Nuth, J. A. *Nature* **1987**, *329*, 589.
(8) Badzian, P.; Verwoerd, S. W.; Ellis, W. P.; Greiner, N. R. *Nature* **1990**, *343*, 244−245.
(9) Hwang, N. M.; Bahng, G. W.; Yoon, D. N. *Diamond Relat. Mater*. **1992**, *1*, 191−194.
(10) Gamarnik, M. Y. *Nanostruct. Mater.* **1996**, *7* (6), 651−658.
(11) Ree, F. H.; Winter, N. W.; Glosli, J. N.; Viecelli, J. A. *Phys. B* **1999**, *265*, 223−229.
(12) Barnard, A. S.; Russo, S. P.; Snook, I. K. *Phys. Rev. B* **2003**, *68*, 073406−4.
(13) Jiang, Q.; Chen, Z. P. *Carbon* **2006**, *44* (1), 79−83.
(14) Fedoseev, D. V.; Deryagin, B. V.; Varshavskayu, I. G. *Surf. Coat. Technol*. **1989**, *38*, 1−122.
(15) Staver, A. M.; Gubareva, N. V.; Lyamkin, A. I.; Petrov, E. A. *Fiz. Goreniya Vzryva*, **1984**, *20*, 100−104.
(16) Greiner, N. R.; Phillips, D. S.; Johnson, J. D.; Volk, F. *Nature* **1988**, *333*, 440−442.
(17) Prawer, S.; Peng, J. L.; Orwa, J. O.; McCallum, J. C.; Jamieson, D. N.; Bursill, L. A. *Phys. Rev. B* **2000**, *62* (24), R16360−R16363.
(18) Yusa, H. *Diamond Relat. Mater*. **2002**, *11*, 87−91.
(19) Sun, J.; Lei, Y.; Zhai, Q.; Yang, X.; Yang, J.; Du, X. *Chin. Opt. Lett.* **2005**, *3* (5), 287−288.
(20) Kuznetsov, V. L.; Chuvilin, A. L.; Butenko, Yu.V.; Malkov, I. Yu.; Titov, V. M. *Chem. Phys. Lett*. **1994**, *222*, 343−348.
(21) Butenko, Yu. V.; Kuznetsov, V. L.; Chuvilin, A. L.; Kolomiichuk, V. N.; Stankus, S. V.; Khairulin, R. A.; Segall, B. *J. Appl. Phys*. **2000**, *88* (7), 4380−4388.
(22) Chen, J.; Deng, S. Z.; Chen, J.; Yu, Z. X.; Xu, N. S. *Appl. Phys. Lett*. **1999**, *74* (24), 3651−3653.
(23) Xu, N. S.; Chen, J.; Deng, S. Z. *Diamond Relat. Mater*. **2002**, *11*, 249−256.
(24) Tomita, S.; Burian, A.; Dore, J. C.; LeBolloch, D.; Fujii, M.; Hayashi, S. *Carbon*, **2002**, *40*, 1469−1474.
(25) Tomita, S.; Sakurai, T.; Ohta, H.; Fujii, M.; Hayashi, S. *J. Chem. Phys*. **2001**, *114* (17), 7477−7482.
(26) Qiao, Z.; Li, J.; Zhao, N.; Shi, C.; Nash, P. *Scr. Mater*. **2006**, *54*, 225−229.
(27) Wang, C.; Chen, J.; Yang, G.; Xu, N. *Angew. Chem*. **2005**, *117*, 7580−7584.
(28) Banhart, F.; Ajayan, P. M. *Nature* **1996**, *382*, 433−435.
(29) Wesolowski, P.; Lyutovich, Y.; Banhart, F.; Carstanjen, H. D.; Kronmuller, H. *Appl. Phys. Lett.* **1997**, *71*, 1948−1950.
(30) Wei, B.; Zhang, J.; Liang, J.; Wu, D. *Carbon* **1998**, *36*, 997−1001.
(31) Tomita, S.; Fujii, M.; Hayashi, S.; Yamamoto, K. *Diamond Relat. Mater*. **2000**, *9*, 856−860.
(32) Qian, J.; Pantea, C.; Huang, J.; Zerda, T. W.; Zhao, Y. *Carbon* **2004**, *42*, 2691−2697.
(33) Yushin, G. N.; Osswald, S.; Padalko, V. I.; Bogatyreva, G. P.; Gogotsi, Y. *Diamond Relat. Mater.* **2005**, *14*, 1721−1729.
(34) Khvostantsev, L. G.; Vereshchagin, L. F.; Novikov, A. P. *High Temp. High Press.* **1977**, *9*, 637−639.
(35) Kinoshita, K. *Carbon: electrochemical and physicochemical properties;* John Wiley and Sons: New York, 1988.
(36) Solin, S. A.; Ramdas, A. K. *Phys. Rev. B* **1970**, *1*, 1687−1698.
(37) Richter, H.; Wang, Z. P.; Ley, L. *Solid State Commun.* **1981**, *39*, 625−629.
(38) Ager, J. W., III; Veirs, D. K.; Rosenblatt, G. M. *Phys. Rev. B* **1991**, *43*, 6491−6499.
(39) Yoshikawa, M.; Mori, Y.; Obata, H.; Maegawa, M.; Katagiri, G.; Ishida, H.; Ishitani, A. *Appl. Phys. Lett*. **1995**, *67* (5), 694−696.

(40) Obrazcova, E. D.; Fujii, M.; Hayashi, S.; Kuznetsov, V. L.; Butenko, Y. V.; Chuvilin, A. L. *Carbon* **1998**, *36* (5−6), 821−826.
(41) Mykhaylyk, O. O.; Solonin, Y. M.; Batchelder, D. N.; Brydson, R. *J. Appl. Phys.* **2005**, *97*, 074302−16.
(42) Baranov, A. V.; Bekhterev, A. N.; Bobovich, Y. S.; Petrov, V. I. *Opt. Spectrosc.* **1987**, *62*, 612−618.
(43) Ferrari, A. C.; Robertson, J. *Phys. Rev. B* **2000**, *61*, 14095−14107.
(44) Tuinstra, F.; Koening, J. L. *J. Chem. Phys.* **1970**, *53*, 1126−1130.
(45) Wada, N.; Solin, S. A. *Phys. B* **1981**, *105*, 353−356.
(46) Davydov, V. A.; Rakhmanina, A. V.; Boudou, J.-P.; Thorel, A.; Allouchi, H.; Agafonov, V. *Carbon* **2006**, *44*, 2015−2020.